

Low-Level Accelerations Applied in the Absence of Weight Bearing Can Enhance Trabecular Bone Formation

Russell Garman,¹ Glenn Gaudette,² Leah-Rae Donahue,³ Clinton Rubin,¹ Stefan Judex¹

¹Department of Biomedical Engineering, State University of New York at Stony Brook, Psychology A Building, Third Floor, Stony Brook, New York 11794-2580

²Department of Biomedical Engineering, Worcester Polytechnic Institution, Worcester, Massachusetts 01609

³The Jackson Laboratory, Bar Harbor, Maine

Received 13 February 2006; accepted 31 October 2006

Published online in Wiley InterScience (www.interscience.wiley.com). DOI 10.1002/jor.20354

ABSTRACT: High-frequency whole body vibrations can be osteogenic, but their efficacy appears limited to skeletal segments that are weight bearing and thus subject to the induced load. To determine the anabolic component of this signal, we investigated whether low-level oscillatory displacements, in the absence of weight bearing, are anabolic to skeletal tissue. A loading apparatus, developed to shake specific segments of the murine skeleton without the direct application of deformations to the tissue, was used to subject the left tibia of eight anesthetized adult female C57BL/6J mice to small (0.3 g or 0.6 g) 45 Hz sinusoidal accelerations for 10 min/day, while the right tibia served as an internal control. Video and strain analysis revealed that motions of the apparatus and tibia were well coupled, inducing dynamic cortical deformations of less than three microstrain. After 3 weeks, trabecular metaphyseal bone formation rates and the percentage of mineralizing surfaces (MS/BS) were 88% and 64% greater ($p < 0.05$) in tibiae accelerated at 0.3 g than in their contralateral controls. At 0.6 g, bone formation rates and mineral apposition rates were 66% and 22% greater ($p < 0.05$) in accelerated tibiae. Changes in bone morphology were evident only in the epiphysis, where stimulated tibiae displayed significantly greater cortical area (+8%) and thickness (+8%). These results suggest that tiny acceleratory motions — independent of direct loading of the matrix — can influence bone formation and bone morphology. If confirmed by clinical studies, the unique nature of the signal may ultimately facilitate the stimulation of skeletal regions that are prone to osteoporosis even in patients that are suffering from confinement to wheelchairs, bed rest, or space travel. © 2007 Orthopaedic Research Society. Published by Wiley Periodicals, Inc. J Orthop Res

Keywords: mechanical stimuli; acceleratory motions; deformations; bone formation; cortical bone; trabecular bone; morphology; osteoporosis; mouse

INTRODUCTION

The skeleton may respond to changes in its mechanical environment by altering cellular activity and morphology. Efforts to exploit bone's mechanosensitivity to strengthen the skeleton and to retard diseases such as osteoporosis have involved exercise^{1,2} and external loading^{3,4} regimes, albeit with varying levels of clinical success.^{5,6} Differences in the anabolic and anti-catabolic capacity of different exercise regimes, such as between swimming and high-impact exercise,

have often been attributed to differences in the induced matrix deformation.

In support for the assumption that strain magnitude is the critical parameter driving bone adaptation, either directly or indirectly through byproducts such as strain rate, strain gradients, or fluid flow, the deformation magnitude has been directly associated with the magnitude of the response.^{7–9} It has further been suggested that strain thresholds must be exceeded to achieve a quantifiable response, both at the tissue¹⁰ and the cell¹¹ levels. Mechanical treatments for low bone mass may appear advantageous when compared to pharmaceutical interventions that bear the risk of side effects.^{12–15} But any clinical mechanical intervention that relies on the application of large loads may be infeasible for targeted populations

Correspondence to: Stefan Judex (Telephone: 631-632-1549; Fax: 631-632-8577; E-mail: stefan.judex@sunysb.edu)

© 2007 Orthopaedic Research Society. Published by Wiley Periodicals, Inc.

(e.g., frail elderly, patients confined to bed rest, or patients with low compliance) and might induce the very fractures that it was intended to prevent.

The need to exceed a strain threshold may have interdependent factors, such as the low frequency at which these loading regimens are most typically employed. Recent studies have indicated that even extremely small deformations, at least two orders of magnitude smaller than those previously suggested, can be anabolic to bone when the frequency of the loading stimulus is increased from the commonly applied 0.5 to 3 Hz to above 30 Hz.^{16–19} These stimuli are induced via whole body vibrations (WBV) and, in humans, transmitted to weightbearing bones of the lower extremities and the axial skeleton.²⁰ Emphasizing the mechanical nature of the stimulus, vibrations do not produce systemic skeletal changes, but act in a local, site-specific manner.²¹ Despite successes of WBV in small-scale clinical trials,^{22,23} an apparent limitation is its reliance on weight bearing as only bones of the lower and axial skeleton can be targeted by standing on a vibrating plate. Confining the anabolic response to weightbearing bones excludes skeletons incapable of bearing weight (e.g., patients with spinal injuries or muscular dystrophy) or clinically important sites not associated with weight bearing (e.g., distal radius). Considering that electric fields,^{24,25} intramedullary pressure,²⁶ and ultrasound^{27,28} can all effectively promote bone formation and fracture healing, the direct application of matrix deformations may not be a required component for WBV to be efficacious.

Here, we modified the stimulus delivered by WBV with the goal to develop a novel physical regime that (1) is low in magnitude and safe to apply to even frail skeletons, (2) can be delivered to skeletal segments in the complete absence of weight bearing, and (3) requires a finite amount of time to be efficacious. Specifically, we hypothesized that bone can perceive small high-frequency oscillatory displacements applied to skeletal segments as osteogenic.

MATERIALS AND METHODS

Experimental Design

All procedures were reviewed and approved by the Institutional Animal Care and Use Committee. High-frequency accelerations were applied to the left tibia of eight adult (19 week) female C57BL/6J (B6) mice, while the right tibia served as an intra-animal contralateral control. Ten age-matched B6 mice were assigned to sham controls to test whether the attachment of the acceleratory device itself might induce a response. In

this group, the left tibia was attached to the loading device without the delivery of the signal, and the right tibia served as a contralateral intra-animal control. All animals were housed in individual cages and allowed free access to standard rodent chow and water. Motions were delivered to the tibia as sinusoidal displacements for 5 days/week, 10 min/day at peak accelerations of 0.3 *g* ($n = 4$) or 0.6 *g* ($n = 4$). At a stimulus frequency of 45 Hz, the nominal displacement output of the transducer was 76 μm at 0.3 *g* and 152 μm at 0.6 *g*. To document differences in dynamic indices of bone formation, calcein injections were administered on days 9 and 19 (15 mg/kg, IP); mice were sacrificed on day 21. Four additional mice were used to characterize kinematics ($n = 2$) and deformations ($n = 2$) of the tibial cortical shell during the oscillatory accelerations.

Applications of Oscillatory Accelerations

A device was developed to deliver high-frequency displacements to skeletal segments in the absence of weight bearing (Fig. 1). The apparatus consisted of a transducer (ACS250, Altec Lansing Tech., Inc., Milford, PA) driven by a function generator (DS345, Stanford Reach Systems, Sunnyvale, CA) to control frequency and amplitude of the tibial motion that was applied parallel to its longitudinal axis. The body of the mouse was supported by a height-adjustable bed. During stimulation, the mouse was anesthetized with a gaseous

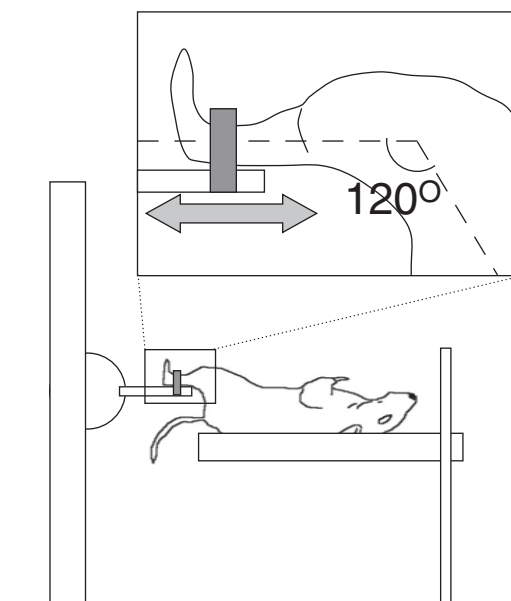


Figure 1. Schematic of the apparatus developed to deliver high-frequency oscillatory motions to the left tibia of a mouse. A transducer (on the left) driven by a function generator produced the accelerations that were transferred to the left tibia via a plastic piece and a strap transverse to it. The insert provides details on the coupling between the horizontally oscillating plastic piece and the tibia. During stimulation, the flexion angle was approximately 120°.

2% isoflurane/oxygen mix. To secure the leg to the plastic attachment of the transducer, the distal portion of the tibia was positioned between two pieces of soft rubber and gently strapped. Longitudinally, the body of the mouse was positioned such that the angle between the tibia and femur was approximately 120° (Fig. 1).

Kinematic Measurements

To determine tibial kinematics during stimulation, each of the two assigned mice was anesthetized (2% isoflurane). The anteromedial tibial surface was exposed through a anterior longitudinal incision on the lower leg and clearing the surface from soft tissues. Accelerations were confirmed by positioning a single-axis accelerometer (CXL04LP1, Crossbow Tech. Inc., San Jose, CA) on the plastic attachment of the transducer (which attached to the tibia). Tibial kinematics during stimulation were determined by high density mapping (HDM) that measured relative displacements between consecutive frames.²⁹ A CMOS camera (Fastcam-X 1280 PCI, Photron USA, Inc., San Diego, CA) recorded images of 320 × 256 pixels at 1,000 frames/s for 5 s.²⁹ Upon dividing the region of interest (ROI) into subimages, phase correlation, based on grayscale intensities within the subimages, was used to calculate displacements occurring in each subimage. This process was repeated until displacements were calculated over the entire ROI for each pair of consecutive frames. The ROI was defined by the available exposed area of the anteromedial surface. The subimage size was 16 × 16 pixels, and the shift of the subimage was 8 pixels. Displacements were calculated as either positive (moving in the direction of the coordinate axis) or negative (moving in opposite direction of the coordinate axis) values. Thus, sampling data at 1,000 Hz for 5 s resulted in 5,000 (relative) displacements values (for a given subimage). The absolute displacement of the ROI at any given time was calculated as the sum of all previous relative displacements. Calculation of the absolute displacements for all frames produced the temporal pattern of the motion.

To calibrate the HDM, transducer accelerations were determined by HDM and compared to the accelerometer readings using the average of four trials at 0.3 g and 0.6 g. Each mouse was subjected to four to six trials. For each trial, the tibia was attached to the device, displacements were recorded from its surface at the defined setting, and then the tibia was detached. Of each 5-s trial, data were analyzed between frames 1,000 and 1,250. Displacement frequency and peak acceleration magnitudes of the sine waves were calculated using a custom MatLab program.

Strain Measurements

At the same anatomical location used for the kinematic measurements, deformations induced by application of oscillatory accelerations were measured in two anesthetized mice with single-element strain gauges (UFLK-1-11-1L, Tokyo Sokki Kenkyujo Co., Ltd, Tokyo, Japan).

Soft tissues were removed, and the gauge was adhered to the bone surface with cyanoacrylate. Strains were recorded during six trials with 45 Hz oscillations at peak accelerations of either 0.3 g or 0.6 g. Strains were also recorded with the function generator set to 0 V output and the tibia either secured to the device ($n = 6$) or unattached ($n = 6$). To test whether the vibration itself might elicit a measurable signal in the gauge, a gauge was attached to a stiff methyl methacrylate block that was vibrated at the prescribed frequency and acceleration.

Strain signals were amplified with low-noise amplifiers (SX500, Beacon Dynamics, Dover, NJ) at a gain of 2,000 and filtered at a cutoff frequency of 200 Hz.³⁰ The signals, recorded at 2000 Hz for 5 s, were digitized at 16-bit resolution. Peak-to-peak strains were calculated for a random 0.25-s period using customized MatLab and Fast Fourier Transform routines.

Bone Morphology and Histomorphometry

Following euthanasia, the lengths of the tibiae were measured using calipers. To assess differences in trabecular (metaphysis and epiphysis) and cortical (epiphysis and mid-diaphysis) bone morphology between stimulated and control tibiae, the proximal and diaphyseal tibia was scanned in a microcomputed tomography scanner (μ CT 40, Scanco Medical, Bassersdorf, Switzerland) at a resolution of 6 μ m (70 kVp, 114 mA).³¹ The epiphyseal region was confined at the proximal end by the divergence of the condyles and at the distal end by the growth plate. The metaphyseal region spanned 582 μ m, beginning 390 μ m from the physeal–metaphyseal demarcation; the mid-diaphyseal region encompassed 120 μ m of the central diaphysis. Appropriate thresholds were determined for each region to match cortical and trabecular quantity and connectedness between the segmented and the raw images.³¹ For a given region, the threshold was identical across all bones and mice. For trabecular bone, bone volume within the volume of interest (BV), bone volume fraction (BV/TV), connectivity density (Conn.D), trabecular number (Tb.N), trabecular thickness (Tb.Th), trabecular separation (Tb.Sp), and structural model index (SMI) were determined via software supplied by the manufacturer. Cortical bone was assessed for differences in endocortical envelope area (Ec.En), periosteal envelope area (Ps.En), cortical bone area (Ct.Ar), and cortical thickness (Ct.Th; Fig. 2).

Histomorphometry was used to measure indices of bone formation in the proximal and diaphyseal regions of the left and right tibia in both experimental and sham control animals. Upon μ CT scanning, samples were dehydrated in isopropyl alcohol and infiltrated with a series of three solutions comprising methyl methacrylate (85%), *N*-butyl phthalate (15%), and benzoyl peroxide (increasing in concentration from 0 to 1 to 2 g/100 mL), and then embedded.³² Coronal 7- μ m sections were cut of the proximal tibia on a microtome (Model 2165, Leica Microsystems, Wetzlar, Germany), while 40- μ m transverse mid-diaphyseal sections were cut with a

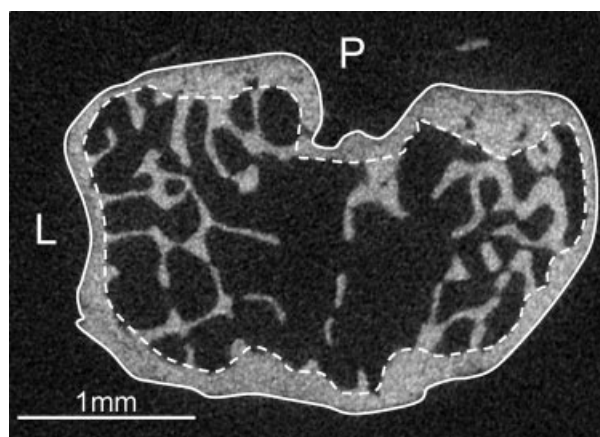


Figure 2. Unprocessed two-dimensional μ CT image from the central epiphysis of the proximal tibia. The area enclosed by the solid line was quantified as the periosteal envelope; the area enclosed by the dotted line was quantified as the endocortical envelope. The difference between the two amounted to the cortical bone area. Limbs subjected to high-frequency oscillations for 10 min/day had a significantly greater cortical bone area and thickness when compared to age-matched controls. Trabecular bone morphology was not affected in this short-term study. Abbreviations: L, lateral; P, posterior.

diamond wire saw (Model 3241, Well Diamond Wire Saws, Inc., Norcross, GA). Metaphyseal trabecular bone and diaphyseal cortical bone were evaluated for differences in the percentage of single labeled surfaces (sLS/BS), double-labeled surfaces (dLS/BS), mineralizing surfaces (MS/BS), mineral apposition rates (MAR), and bone formation rates (BFR/BS) with bone surface (BS) as a referent.³³

Statistics

Differences in bone morphology and formation between the experimental and control tibiae in both experimental and sham control mice were evaluated using a (paired) nonparametric Wilcoxon test (SPSS for Windows 9.0). Differences in bone formation between the right control tibiae of experimental mice and the left and right tibiae of sham controls were tested with a Kruskal–Wallis test. All data were presented as mean \pm standard error (SE), due to the relatively small sample sizes.

RESULTS

Kinematics of the Tibia

Video HDM confirmed that the motion of the anteromedial surface of the proximal tibia followed a sinusoidal 45 Hz wave form (Fig. 3). At nominal 0.3 g peak accelerations, the peak acceleration of the tibia across mice and trials (0.30 ± 0.03 g) was within 0.1% of the acceleration of the plastic attachment. Increasing peak accel-

eration of the transducer to 0.6 g slightly increased this discrepancy, but peak acceleration of the tibia (0.62 ± 0.01 g) stayed within 3% of the peak acceleration of the device.

Strains Induced in the Tibia

At 0.3 g peak accelerations, peak-to-peak strains induced in the proximal tibia were 1.1 ± 0.1 $\mu\epsilon$ (Fig. 3). Doubling peak acceleration to 0.6 g doubled the strains (2.2 ± 0.5 $\mu\epsilon$; Fig. 3). As expected, the predominant strain frequency induced by the acceleratory motions was the signal frequency (45 Hz). Peak deformations that occurred while the tibia was secured to the device without stimulation averaged 0.6 ± 0.2 $\mu\epsilon$, identical to the average generated strains when the leg was not attached to the device (0.6 ± 0.2 $\mu\epsilon$). These latter recordings were not associated with a dominant frequency, except for a spike at 60 Hz (noise of the electric lines). Vibration of the strain gauge itself produced peak strains within the noise range.

Bone Formation and Morphology

High-frequency oscillatory displacements stimulated trabecular bone formation when compared to nonstimulated contralateral controls. Tibiae oscillated at 0.3 g displayed 64% greater MS/BS ($p < 0.05$) and 88% greater BFR/BS ($p < 0.05$) in the metaphysis (Table 1). Tibiae accelerated at 0.6 showed 22% greater MAR ($p < 0.05$) and 66% greater BFR/BS ($p < 0.05$) than the control tibiae (Table 1). When bones from the two groups were pooled (because of the similar response), the pooled accelerated tibiae revealed greater MS/BS (54%, $p < 0.05$) and BFR/BS (78%, $p < 0.05$) than the pooled contralateral controls (Table 1). In cortical bone of the mid-diaphysis, 0.3 g accelerations elevated endocortical MS/BS (20%, $p < 0.05$) and dLS/BS (+56%, $p < 0.05$) as compared to controls (Table 2). At 0.6 g peak accelerations, endocortical MS/BS was 15% smaller ($p < 0.05$) in stimulated limbs (Table 2).

In sham control mice, the left tibia (attached to the device without stimulation) displayed no difference in bone formation indices of metaphyseal trabecular or diaphyseal cortical bone when compared to the contralateral control (Tables 1, 2). No significant differences in bone formation were found among any of the three control groups (contralateral control of experimental mice, left tibia of sham control mice, right contralateral tibia of sham control mice).

After 3 weeks of oscillatory motions for 10 min/day, bone morphology differences between

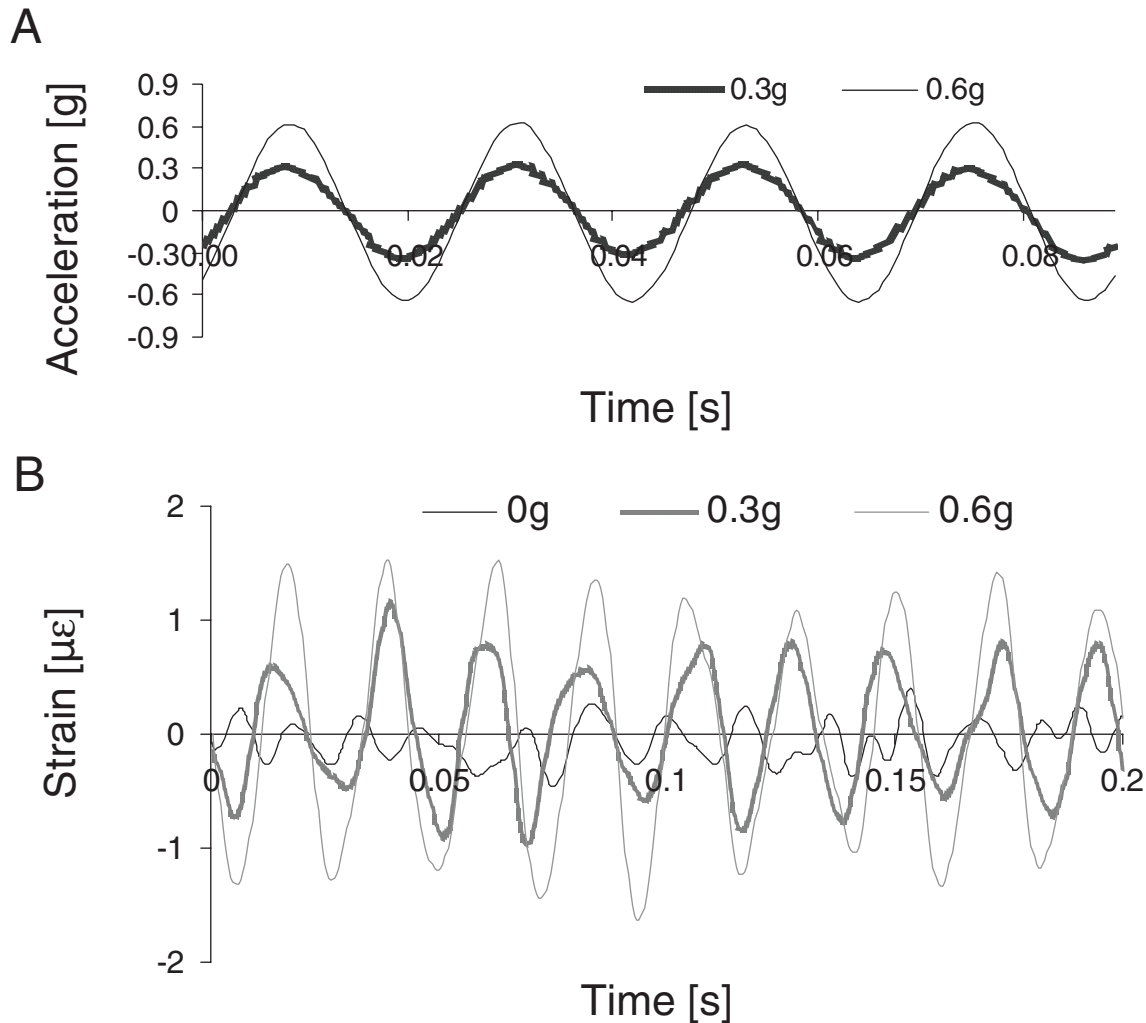


Figure 3. (A) Temporal patterns of the accelerations applied to the proximal tibia, as determined by high density mapping, while peak output accelerations of the transducer were set to either 0.3 g or 0.6 g. (B) Longitudinal normal strains, induced at the anteromedial surface of the proximal tibia, while peak acceleratory motions of the transducer were set to 0 g (leg attached to an inactive transducer), 0.3 g, or 0.6 g.

experimental and control limbs were only detected in epiphyseal cortical bone in which bone area and transcortical thickness were significantly greater. These differences were not significant when considering the two accelerated groups separately, but pooled across animals, bone area was 8.4% ($p < 0.05$) and thickness was 8.2% ($p < 0.05$) greater in accelerated tibiae (Table 3). No significant differences in bone length or trabecular bone morphology were detected between accelerated and control tibiae (Table 4).

DISCUSSION

The anabolic response of bone to low-level WBV has been presumed to be associated with deformations induced in the matrix. In consider-

ing the osteogenic potential of nonmechanical interventions such as electric fields and ultrasound, the necessity to induce the mechanical signal via direct deformations, rather than accelerations, was raised. If the anabolic potential of specific mechanical signals, such as WBV, could be realized in the absence of load bearing, it would help in defining key parameters in bone adaptation and expand the application of using mechanical signals in prevention and treatment of musculoskeletal disorders. To determine if the form-follows-function rules of the skeleton rely critically on load per se, this study sought to answer the question whether bone may be able to sense oscillatory motions directly.

A device was developed to subject the tibia of a mouse to high-frequency motions, producing

Table 1. Static and Dynamic Histomorphometric Indices (Mean \pm SE) of Metaphyseal Trabecular Bone of Tibiae Stimulated at Peak Accelerations of 0.3 g Or 0.6 g, the Pool of the Two Acceleration Groups, Sham Controls, As Well As Their Respective Contralateral Controls

Experimental Group	sLS/BS (%)	dLS/BS (%)	MS/BS (%)	MAR ($\mu\text{m}/\text{day}$)	BFR/BS ($\mu\text{m}^3/\mu\text{m}^2/\text{year}$)
Control (0.3 g)	15.6 \pm 2.7*	7.0 \pm 2.1	14.8 \pm 2.4*	1.1 \pm 0.2	61.1 \pm 19.4*
Accelerated (0.3 g)	27.1 \pm 6.2*	10.8 \pm 3.7	24.3 \pm 3.9*	1.3 \pm 0.2	114.8 \pm 17.2*
Control (0.6 g)	22.8 \pm 5.3	5.4 \pm 1.8	16.8 \pm 3.8	1.1 \pm 0.1*	69.9 \pm 17.4*
Accelerated (0.6 g)	22.8 \pm 3.4	12.4 \pm 2.6	23.8 \pm 3.4	1.4 \pm 0.2*	115.8 \pm 14.0*
Control (pooled)	18.7 \pm 2.9	6.4 \pm 1.3	15.7 \pm 2.0*	1.1 \pm 0.1	64.9 \pm 12.4*
Accelerated (pooled)	24.9 \pm 3.3	11.6 \pm 2.1	24.0 \pm 2.3*	1.3 \pm 0.1	115.3 \pm 9.9*
Control (sham)	17.1 \pm 3.6	4.4 \pm 1.1	15.6 \pm 1.2	0.8 \pm 0.1	47.5 \pm 11.5
Sham	21.0 \pm 4.4	3.1 \pm 0.9	15.8 \pm 2.5	0.9 \pm 0.2	53.0 \pm 13.2

Abbreviations: BFR: bone formation rate; BS: bone surface; dLS: double labeled surface; MAR: mineral apposition rate; MS: mineralizing surface; sLS: single labeled surface.

* $p < 0.05$ between stimulated and control tibiae.

displacements on the order of 100 μm , while leaving the contralateral limb undisturbed. The motion was readily transferred from the transducer to the tibia through a padded strap which, by itself, did not affect levels of bone formation or bone morphology. The accelerations induced cortical bone strains of 1 to 2 microstrain, three orders of magnitude below peak strains during walking, and associated with strains induced in the diaphysis during quiet activities such as standing, presumably induced by postural muscle activity.³⁰ Application of these small stimuli for 10 min/day increased trabecular bone formation in the metaphysis and enhanced cortical bone morphology in the epiphysis. If this novel means of stimulating bone (re)modeling can be extrapolated to humans, the unique nature of the signal may facilitate bone growth in skeletal segments that are prone to bone fragility, even in patients suffering from immobility due to spinal cord injury, incapacitated due to confinement to wheelchairs or bed rest, and who are subject to

reduced activity which might arise during space travel.

When interpreting our results, limitations must be considered. The contralateral design increased statistical power and ensured that the observed differences in bone formation and morphology could be attributed directly to the applied stimulus, but systemic stimuli may have influenced the results. The inclusion of the sham control group eliminated the possibility that either the attachment of the apparatus induced a local response or that shaking of one limb induced a systemic response. It is also unlikely that the low intensity of the electromagnetic field produced by the transducer had the ability to systemically alter cellular activity in the adult skeletal tissue with normal turnover.^{34,35} Even if such an event took place, it could not account for the unilateral effects observed in this study.

The absence of differences in morphology between control and stimulated tibiae in some

Table 2. Static and Dynamic Histomorphometric Indices (Mean \pm SE) of the Mid-Diaphyseal Endocortical Surface of Tibiae Stimulated at Peak Accelerations of 0.3 g or 0.6 g, the Pool of the Two Acceleration Groups, Sham Controls, As Well As Their Respective Contralateral Controls

Experimental Group	sLS/BS (%)	dLS/BS (%)	MS/BS (%)	MAR ($\mu\text{m}/\text{day}$)	BFR/BS ($\mu\text{m}^3/\mu\text{m}^2/\text{year}$)
Control (0.3 g)	42.7 \pm 10.0	26.1 \pm 3.5*	47.5 \pm 4.7*	0.7 \pm 0.2	131.1 \pm 36.0
Accelerated (0.3 g)	31.8 \pm 8.1	40.9 \pm 3.9*	56.8 \pm 3.0*	0.6 \pm 0.1	119.9 \pm 11.5
Control (0.6 g)	37.0 \pm 7.4	30.7 \pm 8.0	49.2 \pm 4.8*	0.6 \pm 0.1	111.1 \pm 20.0
Accelerated (0.6 g)	36.2 \pm 6.0	23.7 \pm 6.9	41.8 \pm 6.6*	0.6 \pm 0.2	96.0 \pm 50.8
Control (pooled)	39.9 \pm 8.3	28.4 \pm 5.8	48.4 \pm 4.4	0.7 \pm 0.1	121.1 \pm 27.5
Accelerated (pooled)	34.0 \pm 6.7	32.3 \pm 7.0	49.3 \pm 6.2	0.6 \pm 0.1	108.0 \pm 34.7
Control (sham)	45.4 \pm 5.8	18.8 \pm 5.2	40.3 \pm 5.8	0.7 \pm 0.1	112.0 \pm 21.2
Sham	34.9 \pm 4.0	23.0 \pm 4.7	40.5 \pm 3.9	0.7 \pm 0.1	98.3 \pm 11.1

Abbreviations: BFR: bone formation rate; BS: bone surface; dLS: double labeled surface; MAR: mineral apposition rate; MS: mineralizing surface; sLS: single labeled surface.

* $p < 0.05$ between stimulated and control tibiae.

Table 3. Morphological Indices (Mean ± SE) of the Epiphyseal and Diaphyseal Cortex of Tibiae Stimulated at Peak Accelerations of 0.3 g or 0.6 g, As Well As for the Pool of the Two Acceleration Groups; Contralateral Tibiae Served as Intra-Animal Controls

Site	Index	Control	0.3 g	Control	0.6 g	Pooled Control	Pooled Stimulated
Epiphysis	Ec.En (mm ²)	3.05 ± 0.05	3.17 ± 0.06	3.15 ± 0.03	2.99 ± 0.06	3.10 ± 0.04	3.08 ± 0.07
	Ps.En (mm ²)	3.84 ± 0.05	4.01 ± 0.08	3.92 ± 0.04	3.84 ± 0.08	3.88 ± 0.05	3.93 ± 0.09
	Ct.Ar (mm ²)	0.79 ± 0.01	0.84 ± 0.03	0.77 ± 0.02	0.85 ± 0.04	0.78 ± 0.02*	0.85 ± 0.03*
	Ct.Th (mm)	121 ± 2	123 ± 1	116 ± 5	131 ± 5	119 ± 1*	128 ± 4*
Diaphysis	Ec.En (mm ²)	0.44 ± 0.01	0.45 ± 0.02	0.44 ± 0.01	0.44 ± 0.01	0.44 ± 0.01	0.44 ± 0.01
	Ps.En (mm ²)	1.10 ± 0.02	1.08 ± 0.02	1.09 ± 0.02	1.10 ± 0.01	1.09 ± 0.01	1.09 ± 0.01
	Ct.Ar (mm ²)	0.66 ± 0.02	0.64 ± 0.01	0.65 ± 0.02	0.65 ± 0.01	0.65 ± 0.01	0.64 ± 0.01
	Ct.Th (mm)	216 ± 5	211 ± 4	215 ± 3	215 ± 5	215 ± 3	213 ± 3

Abbreviations: Ct.Ar: cortical bone area; Ct.Th: cortical thickness; Ec.En: endocortical envelope area; Ps.En: periosteal envelope area.

**p* < 0.05 between stimulated and control tibiae.

anatomical regions, despite altered indices of bone formation, is consistent with other short-term mechanical (un)loading studies of the adult rodent skeleton,^{3,4,17,36} in part reflecting the low levels of normal bone turnover in many genetic strains, requiring loading durations in excess of 3 weeks to establish morphological changes. The small samples sizes used in this study had sufficient statistical power to show the initial proof of concept for using accelerations, but further investigations will be required to explore the mechanisms by which bone can sense oscillations this small, whether the signal is effective in other species including humans, or whether the changes in bone's cellular

activity produce a structure more resistant to fracture. Interestingly, preliminary data from a follow-up study indicate that greater bone formation rates in oscillated limbs can confer significant structural and mechanical benefits to trabecular bone.³⁷

If application of high-frequency oscillations indeed produces a robust anabolic response in trabecular and cortical bone of non-weightbearing bones, it may provide nonpharmacological alternatives to treating low bone mass, in particular in patients who cannot subject their skeletons to normal weight bearing. It also raises the question of how such a small stimulus can be detected. The

Table 4. Morphological Indices (Mean ± SE) of the Trabecular Epiphysis and Metaphysis of Tibiae Stimulated at Peak Accelerations of 0.3 g or 0.6 g, As Well As for the Pool of the Two Acceleration Groups; Contralateral Tibiae Served as Intra-Animal Controls

Site	Index	Control	0.3 g	Control	0.6 g	Pooled Control	Pooled Stimulated
Epiphysis	BV	0.12 ± 0.01	0.12 ± 0.01	0.13 ± 0.01	0.11 ± 0.01	0.12 ± 0.01	0.12 ± 0.01
	BV/TV	0.24 ± 0.01	0.22 ± 0.01	0.24 ± 0.01	0.22 ± 0.01	0.24 ± 0.01	0.22 ± 0.01
	Conn.D.	140.9 ± 10.9	120.5 ± 8.3	139.3 ± 10.3	124.0 ± 10.3	140.1 ± 7.4	122.2 ± 6.6
	SMI	0.51 ± 0.07	0.70 ± 0.06	0.64 ± 0.10	0.71 ± 0.08	0.57 ± 0.07	0.71 ± 0.05
	Tb.N	9.42 ± 1.49	8.37 ± 0.34	8.56 ± 1.76	8.28 ± 0.97	8.99 ± 1.15	8.32 ± 0.51
	Tb.Th	0.06 ± 0.01	0.06 ± 0.01	0.06 ± 0.01	0.06 ± 0.01	0.06 ± 0.01	0.06 ± 0.01
	Tb.Sp	0.14 ± 0.02	0.14 ± 0.01	0.15 ± 0.02	0.15 ± 0.01	0.15 ± 0.01	0.15 ± 0.01
Metaphysis	BV	0.05 ± 0.01	0.04 ± 0.01	0.06 ± 0.01	0.06 ± 0.01	0.05 ± 0.01	0.05 ± 0.01
	BV/TV	0.05 ± 0.01	0.05 ± 0.01	0.06 ± 0.01	0.06 ± 0.01	0.05 ± 0.01	0.05 ± 0.01
	Conn.D.	20.6 ± 2.7	15.8 ± 4.5	22.1 ± 5.5	27.7 ± 2.7	21.4 ± 3.1	21.7 ± 3.5
	SMI	2.52 ± 0.09	2.67 ± 0.14	2.38 ± 0.17	2.49 ± 0.13	2.45 ± 0.10	2.58 ± 0.10
	Tb.N	3.44 ± 0.03	3.46 ± 0.10	3.63 ± 0.03	3.56 ± 0.03	3.54 ± 0.05	3.51 ± 0.05
	Tb.Th	0.04 ± 0.01	0.04 ± 0.01	0.04 ± 0.01	0.04 ± 0.01	0.04 ± 0.01	0.04 ± 0.01
	Tb.Sp	0.29 ± 0.01	0.29 ± 0.01	0.27 ± 0.01	0.28 ± 0.01	0.28 ± 0.01	0.28 ± 0.01

Abbreviations: BV: bone volume; BV/TV: bone volume fraction; Conn.D: connectivity density; Tb.N: trabecular number; Tb.Th: trabecular thickness; Tb.Sp: trabecular separation; SMI: structural model index.

differential response to high-frequency oscillations between different anatomical regions suggests that recognition of the accelerations occurred through a tissue-level mechanism. However, the extremely small induced deformations were close to background strains and resembled those associated with postural muscle activity, clearly questioning the previously suggested thresholds for enhancing anabolic activity.³⁸ Compared to WBV, a low-level mechanical stimulus with anabolic and anti-catabolic potential,^{16,39} the strains induced by oscillatory motions were nearly an order of magnitude smaller ($10 \mu\epsilon$) for the same acceleration and frequency in this mouse model.³⁹ Here, oscillatory motions were not directly contrasted to WBV in their efficacy to alter bone formation and morphology, but the large strain reduction provided further evidence⁴⁰ that matrix strains are unlikely driving bone's response to vibrations.

The distinct adaptive phenomena of bone to either extremely small-magnitude, high-frequency stimuli or much larger magnitude, low-frequency mechanical stimuli suggests alternative pathways by which bone cells detect physical signals. For example, accelerations may generate drag forces that perturb osteocytic processes in the pericellular matrix,⁴¹ providing a strong amplification mechanism for even very small mechanical events.⁴² However, cells might respond to vibrations even in absence of their native environment *in vitro*,^{43,44} perhaps modulated by oscillations of the nucleus in the cytoplasm.⁴⁵ Nevertheless, a generic cell response to vibrations is inconsistent with the site-specific responses observed here, and mechanical factors could interact with physiological (e.g., altered blood flow^{46–48}) and cellular (e.g., cell communication⁴⁹) factors to define the tissue-level response.

In summary, these data demonstrate that extremely low-level, high-frequency oscillations, in the absence of loads applied directly to the matrix, can be osteogenic to bone tissue. This response occurred in the presence of cortical strains that were similar to those levels associated with breathing, blood flow, and background noise, providing further evidence that mechanisms independent of matrix deformation may be critical to bone maintenance and regulation of remodeling, and that omnipresent activities such as standing may provide central regulatory signals to the skeleton independent of bone strain. Further studies are needed to establish and optimize this stimulus, but its unique, non-weightbearing nature may ultimately serve as an effective intervention for the prevention of bone loss in non-

weightbearing skeletal sites or in patients whose skeletons are incapable of bearing weight, such as during bed rest or space flight.

ACKNOWLEDGMENTS

Financial support from the Whitaker Foundation (SJ), the Wallace H. Coulter Foundation (SJ), the National Science Foundation (SJ), NIAMS (CTR), and The Department of the Army (LRD) is gratefully acknowledged. Technical advice from Dr. Mitchell Schaffler, Evren Azeloglu, and Damon Kelly was greatly appreciated. The authors have no conflict of interest.

REFERENCES

1. Friedlander AL, Genant HK, Sadowsky S, et al. 1995. A two-year program of aerobics and weight training enhances bone mineral density of young women. *J Bone Miner Res* 10:574–585.
2. Honda A, Umemura Y, Nagasawa S. 2001. Effect of high-impact and low-repetition training on bones in ovariectomized rats. *J Bone Miner Res* 16:1688–1693.
3. Tanaka SM, Alam IM, Turner CH. 2003. Stochastic resonance in osteogenic response to mechanical loading. *FASEB J* 17:313–314.
4. Lamothe JM, Zernicke RF. 2004. Rest insertion combined with high-frequency loading enhances osteogenesis. *J Appl Physiol* 96:1788–1793.
5. Torvinen S, Kannus P, Sievanen H, et al. 2003. Effect of 8-month vertical whole body vibration on bone, muscle performance, and body balance: a randomized controlled study. *J Bone Miner Res* 18:876–884.
6. Pruitt LA, Taaffe DR, Marcus R. 1995. Effects of a one-year high-intensity versus low-intensity resistance training program on bone mineral density in older women. *J Bone Miner Res* 10:1788–1795.
7. Rubin CT, Lanyon LE. 1985. Regulation of bone mass by mechanical strain magnitude. *Calcif Tissue Int* 37:411–417.
8. Mosley JR, March BM, Lynch J, et al. 1997. Strain magnitude related changes in whole bone architecture in growing rats. *Bone* 20:191–198.
9. Cullen DM, Smith RT, Akhter MP. 2001. Bone-loading response varies with strain magnitude and cycle number. *J Appl Physiol* 91:1971–1976.
10. Hsieh YF, Robling AG, Ambrosius WT, et al. 2001. Mechanical loading of diaphyseal bone *in vivo*: the strain threshold for an osteogenic response varies with location. *J Bone Miner Res* 16:2291–2297.
11. Owan I, Burr DB, Turner CH, et al. 1997. Mechanotransduction in bone: osteoblasts are more responsive to fluid forces than mechanical strain. *Am J Physiol* 273:C810–C815.
12. Mashiba T, Hirano T, Turner CH, et al. 2000. Suppressed bone turnover by bisphosphonates increases microdamage accumulation and reduces some biomechanical properties in dog rib. *J Bone Miner Res* 15:613–620.
13. Reid IR. 2002. Pharmacotherapy of osteoporosis in postmenopausal women: focus on safety. *Expert Opin Drug Safety* 1:93–107.

14. Daly E, Vessey MP, Hawkins MM, et al. 1996. Risk of venous thromboembolism in users of hormone replacement therapy. *Lancet* 348:977–980.
15. Lacey JV Jr, Mink PJ, Lubin JH, et al. 2002. Menopausal hormone replacement therapy and risk of ovarian cancer. *JAMA* 288:334–341.
16. Rubin C, Turner AS, Bain S, et al. 2001. Anabolism: low mechanical signals strengthen long bones. *Nature* 412: 603–604.
17. Rubin C, Xu G, Judex S. 2001. The anabolic activity of bone tissue, suppressed by disuse, is normalized by brief exposure to extremely low-magnitude mechanical stimuli. *FASEB J* 15:2225–2229.
18. Oxlund BS, Ortoft G, Andreassen TT, et al. 2003. Low-intensity, high-frequency vibration appears to prevent the decrease in strength of the femur and tibia associated with ovariectomy of adult rats. *Bone* 32:69–77.
19. Midura RJ, Dillman CJ, Grabiner MD. 2005. Low amplitude, high frequency strains imposed electrically stimulated skeletal muscle retards the development of osteopenia in the tibiae of hindlimb suspended rats. *Med Eng Phys* 27:285–293.
20. Rubin C, Pope M, Fritton JC, et al. 2003. Transmissibility of 15-hertz to 35-hertz vibrations to the human hip and lumbar spine: determining the physiologic feasibility of delivering low-level anabolic mechanical stimuli to skeletal regions at greatest risk of fracture because of osteoporosis. *Spine* 28:2621–2627.
21. Rubin C, Turner AS, Mallinckrodt C, et al. 2002. Mechanical strain, induced noninvasively in the high-frequency domain, is anabolic to cancellous bone, but not cortical bone. *Bone* 30:445–452.
22. Rubin C, Recker R, Cullen D, et al. 2004. Prevention of postmenopausal bone loss by a low-magnitude, high-frequency mechanical stimuli: a clinical trial assessing compliance, efficacy, and safety. *J Bone Miner Res* 19:343–351.
23. Ward K, Alsop C, Caulton J, et al. 2004. Low magnitude mechanical loading is osteogenic in children with disabling conditions. *J Bone Miner Res* 19:360–369.
24. Rubin J, McLeod KJ, Titus L, et al. 1996. Formation of osteoclast-like cells is suppressed by low frequency, low intensity electric fields. *J Orthop Res* 14:7–15.
25. McLeod KJ, Rubin CT. 1992. The effect of low-frequency electrical fields on osteogenesis [published erratum appears in *J Bone Joint Surg [Am]* 1992; 74: 1274]. *J Bone Joint Surg [Am]* 74:920–929.
26. Qin YX, Kaplan T, Saldanha A, et al. 2003. Fluid pressure gradients, arising from oscillations in intramedullary pressure, is correlated with the formation of bone and inhibition of intracortical porosity. *J Biomech* 36:1427–1437.
27. Dyson M, Brookes M. 1983. Stimulation of bone repair by ultrasound. *Ultrasound Med Biol Suppl* 2:61–66.
28. Azuma Y, Ito M, Harada Y, et al. 2001. Low-intensity pulsed ultrasound accelerates rat femoral fracture healing by acting on the various cellular reactions in the fracture callus. *J Bone Miner Res* 16:671–680.
29. Kelly DJ, Azeloglu EU, Kochupura PV, et al. 2005. Accuracy and reproducibility of a subpixel extended phase correlation method to determine micron level displacements in the heart. *Med Eng Phys* 29:154–162.
30. Fritton SP, McLeod KJ, Rubin CT. 2000. Quantifying the strain history of bone: spatial uniformity and self-similarity of low-magnitude strains. *J Biomech* 33:317–325.
31. Judex S, Garman R, Squire M, et al. 2004. Genetically based influences on the site-specific regulation of trabecular and cortical bone morphology. *J Bone Miner Res* 19:600–606.
32. Yang LC, Majeska RJ, Laudier DM, et al. 2005. High-dose risedronate treatment partially preserves cancellous bone mass and microarchitecture during long-term disuse. *Bone* 37:287–295.
33. Parfitt AM, Drezner MK, Glorieux FH, et al. 1987. Bone histomorphometry: standardization of nomenclature, symbols, and units. Report of the ASBMR Histomorphometry Nomenclature Committee. *J Bone Miner Res* 2:595–610.
34. Aaron RK, Ciombor DM, Jolly G. 1989. Stimulation of experimental ossification by low-energy pulsing electromagnetic fields. *J Bone Miner Res* 4:227–233.
35. Fredericks DC, Nepola JV, Baker JT, et al. 2000. Effects of pulsed electromagnetic fields on bone healing in a rabbit tibial osteotomy model. *J Orthop Trauma* 14:93–100.
36. Judex S, Donahue LR, Rubin C. 2002. Genetic predisposition to low bone mass is paralleled by an enhanced sensitivity to signals anabolic to the skeleton. *FASEB J* 16:1280–1282.
37. Ozcivici E, Garman R, Rubin C, et al. 2006. Micro-mechanical adaptations of trabecular bone to small amplitude oscillations. *J Bone Miner Res* 20:48.
38. Frost HM. 1990. Skeletal structural adaptations to mechanical usage (SATMU): 1. Redefining Wolff's law: the bone modeling problem. *Anat Rec* 226:403–413.
39. Xie L, Jacobson JM, Choi ES, et al. 2006. Low-level mechanical vibrations can influence bone resorption and bone formation in the growing skeleton. *Bone* 39:1059–1066.
40. Judex S, Lei X, Han D, et al. 2006. Low-magnitude mechanical signals that stimulate bone formation in the ovariectomized rat are dependent on the applied frequency but not on the strain magnitude. *J Biomech* (June 29 E pub ahead of print).
41. Han Y, Cowin SC, Schaffler MB, et al. 2004. Mechanotransduction and strain amplification in osteocyte cell processes. *Proc Natl Acad Sci U S A* 101:16689–16694.
42. You L, Cowin SC, Schaffler MB, et al. 2001. A model for strain amplification in the actin cytoskeleton of osteocytes due to fluid drag on pericellular matrix. *J Biomech* 34: 1375–1386.
43. Tanaka SM, Li J, Duncan RL, et al. 2003. Effects of broad frequency vibration on cultured osteoblasts. *J Biomech* 36:73–80.
44. Tjandrawinata RR, Vincent VL, Hughes-Fulford M. 1997. Vibrational force alters mRNA expression in osteoblasts. *FASEB J* 11:493–497.
45. Bacabac RG, Smit TH, Van Loon JJ, et al. 2006. Bone cell responses to high-frequency vibration stress: does the nucleus oscillate within the cytoplasm? *FASEB J* 20:858–864.
46. Shin S, Ku Y, Suh JS, et al. 2003. Characteristics of blood flow resistance under transverse vibration: red blood cell suspension in Dextran-40. *Ann Biomed Eng* 31:1077–1083.
47. Murfee WL, Hammett LA, Evans C, et al. 2005. High-frequency, low-magnitude vibrations suppress the number of blood vessels per muscle fiber in mouse soleus muscle. *J Appl Physiol* 98:2376–2380.
48. Parfitt AM. 2000. The mechanism of coupling: a role for the vasculature. *Bone* 26:319–323.
49. Ausk BJ, Gross TS, Srinivasan S. 2005. An agent based model for real-time signaling induced in osteocytic networks by mechanical stimuli. *J Biomech* 39:2638–2646.